Numer. Math. Theor. Meth. Appl.
doi: 10.4208/nmtma.2013.y11038

Vol. **6**, No. 2, pp. 325-342
May 2013

A New Discontinuous Galerkin Method for Parabolic Equations with Discontinuous Coefficient

Rongpei Zhang[1,*], Xijun Yu[2], Xia Cui[2], Xiaohan Long[3] and Tao Feng[2]

[1] *School of Sciences, Liaoning Shihua University, Fushun 113001, Liaoning, China.*
[2] *National Key Laboratory of Science and Technology on Computational Physics, Institute of Applied Physics and Computational Mathematics, Beijing 100088, China.*
[3] *School of Mathematics and Information, Ludong University, Yantai 264025, Shandong, China.*

Received 10 October 2011; Accepted (in revised version) 19 August 2012

Available online 12 April 2013

Abstract. In this paper, a new discontinuous Galerkin method is developed for the parabolic equation with jump coefficients satisfying the continuous flow condition. Theoretical analysis shows that this method is L^2 stable. When the finite element space consists of interpolative polynomials of degrees k, the convergent rate of the semi-discrete discontinuous Galerkin scheme has an order of $\mathcal{O}(h^k)$. Numerical examples for both 1-dimensional and 2-dimensional problems demonstrate the validity of the new method.

AMS subject classifications: 65M60, 35K05

Key words: Parabolic equation, discontinuous coefficient, discontinuous Galerkin method, error estimate, stability analysis.

1. Introduction

The parabolic equations with discontinuous coefficients play a great role in many physical applications. For example, in the numerical simulation of radiation hydrodynamics, since energy is usually transported in a variety of media, the conductivity coefficients are discontinuous on the media interface. Sometimes the conductivity coefficients are with several quantity differences. Therefore, it is of great theoretical significance and practical value to study the numerical methods with high order accuracy [1]. There have been some works for solving parabolic problems with discontinuous coefficients by finite difference methods, finite volume methods, and finite element methods. Samarskii [2] studied

*Corresponding author. *Email addresses:* rongpeizhang@163.com (R. P. Zhang), yuxj@iapcm.ac.cn (X. J. Yu), cui_xia@iapcm.ac.cn (X. Cui), long669@163.com (X. H. Long), fengtao2@mail.ustc.edu.cn (T. Feng)

the classical θ-scheme. Shashkov [3] developed support-operators method to solve diffusion equations with rough coefficients. Zhu et al. [4] presented explicit/implicit schemes. Sinha et al. [5] studied the error estimates of finite element method. Huang and Li [6] gave the immersed methods combined with finite difference method and Ewing et al. [7] and Li et al. [8] combined immersed methods with finite element approximations to obtain the numerical solution of the interface problem. The Discontinuous Galerkin (DG) method was first introduced by Reed and Hill [9] for solving neutron transport problems. A major development of the DG method was carried out by Cockburn and Shu [10–13] for solving hyperbolic conservation laws. It now becomes an active research area for solving hyperbolic, elliptic and parabolic equations. The DG method uses a completely discontinuous piecewise polynomial as the solution and test function space, and it has the good properties: local conservation on each element, suitability for hp-adaptive implementation; easily treating rough coefficient problems and effectively capturing discontinuities. For time-dependent convection diffusion problems, DG methods provide substantial computational advantages if explicit time integrations are used. Motivated by the successful realization in solving hyperbolic equations, the DG method is applied to solve equations with high order derivatives and developed as the local discontinuous Galerkin (LDG) method [14], the DG method based on dGRP flux (diffusive generalized Riemann problem) [15,16], and direct discontinuous Galerkin (DDG) method [17, 18]. In recent years, the DG methods have been applied to solve the elliptic equations and advection-diffusion equations with discontinuous coefficients. Ern et al. [19–21] developed a (symmetric) weighted interior penalty (WIP) method which replaces the arithmetic mean with suitably weighted averages where the weights depend on the coefficients of the problem. Cai et al. [22] proposed three different weight averages and established a priori and a posteriori error estimates.

The present paper based on the continuous flow condition constructs a new discontinuous Galerkin method which satisfies the consistent numerical flux. The new DG method needs not introduce auxiliary variables and has high efficiency compared with the LDG method. In meantime, the new DG method can ensure high accuracy and stability and sharply capture the contacts with discontinuous derivatives.

The paper is organized as follows. In Section 2, we construct the new DG scheme for one-dimensional heat conduction equation with jump coefficient and prove the L^2 stability and error estimate. In Section 3, this DG method is extended to two-dimensional heat conduction equation. The stability and convergence analysis are studied. Numerical examples are presented in Section 4 to illustrate the efficiency and accuracy of the new method. Some conclusions are given in the last section.

2. DG scheme for 1D problem

Consider the 1D heat conduction equation:

$$\rho c\frac{\partial U}{\partial t}-\frac{\partial}{\partial x}\Big(\kappa(x)\frac{\partial U}{\partial x}\Big)=f(x,t),\quad x_L<x<x_R,\quad t>0 \tag{2.1}$$

with boundary conditions,

$$a_1U - b_1\kappa(x)\frac{\partial U}{\partial x} = g_1, \quad x = x_L; \quad a_2U - b_2\kappa(x)\frac{\partial U}{\partial x} = g_2, \quad x = x_R$$

and initial condition,

$$U(x,0) = U_0(x).$$

The conductive coefficient $\kappa(x) \geq \kappa_0 > 0$, ρ is medium density, c is specific heat and $f(x,t)$ is the source term. We take $\rho = 1$, $c = 1$ for simplicity. When $b_1 = b_2 = 0$, Eq. (2.1) has the Dirichlet boundary conditions and $a_1 = a_2 = 0$ corresponds to the Neumann boundary conditions. Otherwise Eq. (2.1) has been called with Robin boundary conditions. Assume that $\kappa(x)$ has discontinuity at $x = \xi \in (x_L, x_R)$ and holds

$$\kappa(\xi^-)\frac{\partial U}{\partial x}(\xi^-,t) = \kappa(\xi^+)\frac{\partial U}{\partial x}(\xi^+,t). \tag{2.2}$$

Then the problem (2.1) has a unique weak solution $U(x,t)$, which is smooth on $[x_L,\xi]\times[0,T]$ and $[\xi,x_R]\times[0,T]$ respectively, and satisfy the joint condition

$$U(\xi^-,t) = U(\xi^+,t), \quad \kappa(\xi^-)\frac{\partial U}{\partial x}(\xi^-,t) = \kappa(\xi^+)\frac{\partial U}{\partial x}(\xi^+,t). \tag{2.3}$$

2.1. DG scheme

The computational domain $[x_L,x_R]$ is divided into N uniform elements, $x_L = x_{\frac{1}{2}} < x_{\frac{3}{2}} < \cdots < x_{N+\frac{1}{2}} = x_R$, and the discontinuity point $x = \xi$ typically falls on one grid points. Denote the cell by $I_j = (x_{j-\frac{1}{2}}, x_{j+\frac{1}{2}})$ with the cell center $x_j = (x_{j-\frac{1}{2}} + x_{j+\frac{1}{2}})/2$ and the size of cell $\Delta x = (x_R - x_L)/N$. The DG approximation space is defined as

$$V_h = \left\{ v : v \in P^k(I_j),\ x \in I_j,\ j = 1,\cdots,N \right\}, \tag{2.4}$$

where $P^k(I_j)$ is the set of polynomials of degree less than or equal to k. Here we restrict Eq. (2.1) with Robin boundary conditions and assume $b_1 = b_2 = 1$, $a_1 > 0$, $a_2 > 0$. It can be easily extended to other boundary conditions. The semi-discrete DG scheme of Eq. (2.1) is defined as follows: Find $u \in V_h$ such that, for all test functions $v \in V_h$, there are

$$\int_{I_j} u_t v dx + \int_{I_j} \kappa(x) u_x v_x dx - (\hat{h}(u)v^-)_{j+\frac{1}{2}} + (\hat{h}(u)v^+)_{j-\frac{1}{2}} = \int_{I_j} f v dx, \tag{2.5a}$$

$$\int_{I_j} u(x,0) v dx = \int_{I_j} U_0(x) v dx. \tag{2.5b}$$

The "hat" terms in (2.5) are numerical fluxes, which are single-valued functions defined at the cell interfaces and depend on the discontinuous numerical solutions from both sides

of the interface. Referring to the paper [16], the numerical flux is defined on interior interface,

$$\hat{h}(u)_{j+\frac{1}{2}} = \frac{\beta_0}{\Delta x}(\alpha[u])_{j+\frac{1}{2}} + (\beta(\kappa^- u_x^-) + \gamma(\kappa^+ u_x^+))_{j+\frac{1}{2}}, \quad j = 1, \cdots, N-1, \tag{2.6}$$

and on boundary points,

$$\hat{h}(u)_{\frac{1}{2}} = a_1 u(x_L^+, t) - g_1(t), \quad \hat{h}(u)_{N+\frac{1}{2}} = g_2(t) - a_2 u(x_R^-, t),$$

where

$$\alpha_{j+\frac{1}{2}} = \frac{\sqrt{\kappa_j \kappa_{j+1}}}{\sqrt{\kappa_j} + \sqrt{\kappa_{j+1}}} \max(\sqrt{\kappa_j}, \sqrt{\kappa_{j+1}}),$$
$$\beta_{j+\frac{1}{2}} = \frac{\sqrt{\kappa_{j+1}}}{\sqrt{\kappa_j} + \sqrt{\kappa_{j+1}}}, \quad \gamma_{j+\frac{1}{2}} = \frac{\sqrt{\kappa_j}}{\sqrt{\kappa_j} + \sqrt{\kappa_{j+1}}},$$

β_0 is a positive constant, $\kappa_j = \kappa(x_j)$. The jump at interface $x_{j+\frac{1}{2}}$ is defined as $[u]_{j+\frac{1}{2}} = (u^+ - u^-)_{j+\frac{1}{2}}$.

This numerical flux (2.6) has the following desired properties: (i) it is consistent with the analytical solution; (ii) it is conservative in the sense of being single-valued at interface; (iii) it ensures the L^2-stability; and (iv) it contributes to the high accuracy of the method. Property (i) is satisfied by the joint condition (2.3). Property (ii) is also easily satisfied by the definition of the numerical flux (2.6). In the next section we will prove properties (iii) and (iv).

2.2. Time discretization

We get the ordinary differential equation systems after DG space discretization of the Eq. (2.1)

$$\frac{d}{dt}\mathbf{U}_h = L(\mathbf{U}_h, t). \tag{2.7}$$

The system (2.7) is discretized in time by third-order SSP Runge-Kutta method as follows [23]:

$$\mathbf{U}_h^{(1)} = \mathbf{U}_h^n + \Delta t L(\mathbf{U}_h^n, t^n), \tag{2.8a}$$
$$\mathbf{U}_h^{(2)} = \frac{3}{4}\mathbf{U}_h^n + \frac{1}{4}\mathbf{U}_h^{(1)} + \frac{1}{4}\Delta t L(\mathbf{U}_h^{(1)}, t^n + \Delta t), \tag{2.8b}$$
$$\mathbf{U}_h^{(3)} = \frac{1}{3}\mathbf{U}_h^n + \frac{2}{3}\mathbf{U}_h^{(2)} + \frac{2}{3}\Delta t L\Big(\mathbf{U}_h^{(2)}, t^n + \frac{1}{2}\Delta t\Big). \tag{2.8c}$$

2.3. The stability analysis

For simplicity, set $\tilde{\kappa}_j = \max_{x\in I_j}\kappa(x)$, $\kappa_j^* = \min_{x\in I_j}\kappa(x)$, $\tilde{\kappa} = \max_{j=1,\cdots,N}\tilde{\kappa}_j$, and define norm:

$$\|u\|_{I_j}^2 = \int_{I_j} u^2 dx, \quad |||u|||^2 = \sum_{j=1}^{N} \|u\|_{I_j}^2.$$

Summing up for the equalities (2.5) over $j = 1,\cdots,N$ and integrating over $[0,T]$, we have the following identity:

$$B(u,v) = L(v), \quad \forall v \in V_h, \tag{2.9}$$

where

$$\begin{aligned} B(u,v) = &\int_0^T \left(\sum_{j=1}^{N} \int_{I_j} u_t v dx + \sum_{j=1}^{N} \int_{I_j} \kappa(x) u_x v_x dx + \sum_{j=1}^{N-1} (\hat{h}(u)[v])_{j+\frac{1}{2}} \right) dt \\ &+ \int_0^T \left(a_1 u(x_L^+,t) v(x_L^+,t) + a_2 u(x_R^-,t) v(x_R^-,t) \right) dt, \\ L(v) = &\int_0^T \left(\sum_{j=1}^{N} \int_{I_j} f v dx dt + \int_0^T (g_1 v(x_L^+,t) + g_2 v(x_R^-,t)) \right) dt. \end{aligned}$$

We have the following trace inequalities:

$$|(u_x^-)_{j+\frac{1}{2}}| \le \frac{C}{\sqrt{\Delta x}} \|u_x\|_{I_j}, \quad |(u_x^+)_{j+\frac{1}{2}}| \le \frac{C}{\sqrt{\Delta x}} \|u_x\|_{I_{j+1}}, \tag{2.10}$$

where C is a constant independent of Δx and u. Throughout C is used to denote a generic positive constant, not necessarily the same at each occurrence.

To prove the L^2-stability, we set $v = u$ in (2.9) and get

$$B(u,u) = L(u), \tag{2.11}$$

where

$$\begin{aligned} B(u,u) = &\frac{1}{2}(|||u(\cdot,T)|||^2 - |||u(\cdot,0)|||^2) + \int_0^T \left(\sum_{j=1}^{N} \int_{I_j} \kappa(x) u_x^2 dx \right. \\ &\left. + \sum_{j=1}^{N-1} (\hat{h}(u)[u])_{j+\frac{1}{2}} \right) dt + \int_0^T \left(a_1 u^2(x_L^+,t) + a_2 u^2(x_R^-,t) \right) dt. \end{aligned} \tag{2.12}$$

By using the numerical flux (2.6) and trace inequalities (2.10), we have:

$$
\begin{aligned}
&(\hat{h}(u)[u])_{j+\frac{1}{2}} \\
=&\frac{\beta_0}{\Delta x}(\alpha[u]^2)_{j+\frac{1}{2}} + \left(\beta(\kappa^- u_x^-) + \gamma(\kappa^+ u_x^+)\right)_{j+\frac{1}{2}}[u]_{j+\frac{1}{2}} \\
\geq&\frac{\beta_0}{\Delta x}(\alpha[u]^2)_{j+\frac{1}{2}} - \frac{C}{\sqrt{\Delta x}}\left(\beta_{j+\frac{1}{2}}\tilde{\kappa}_j\|u_x\|_{I_j} + \gamma_{j+\frac{1}{2}}\tilde{\kappa}_{j+1}\|u_x\|_{I_{j+1}}\right)|[u]_{j+\frac{1}{2}}| \\
\geq&\frac{\beta_0}{\Delta x}(\alpha[u]^2)_{j+\frac{1}{2}} - \frac{C}{\sqrt{\Delta x}}\frac{\sqrt{\tilde{\kappa}_j\tilde{\kappa}_{j+1}}}{\sqrt{\kappa_j}+\sqrt{\kappa_{j+1}}}\left(\sqrt{\tilde{\kappa}_j}\|u_x\|_{I_j} + \sqrt{\tilde{\kappa}_{j+1}}\|u_x\|_{I_{j+1}}\right)|[u]_{j+\frac{1}{2}}| \\
\geq&\frac{\beta_0}{\Delta x}(\alpha[u]^2)_{j+\frac{1}{2}} - \frac{2C}{\sqrt{\Delta x}}\sigma_{j+\frac{1}{2}}\left(\tilde{\kappa}_j\|u_x\|_{I_j}^2 + \tilde{\kappa}_{j+1}\|u_x\|_{I_{j+1}}^2\right)^{\frac{1}{2}}|[u]_{j+\frac{1}{2}}|,
\end{aligned}
$$

where $\sigma_{j+\frac{1}{2}} = \sqrt{\tilde{\kappa}_j\tilde{\kappa}_{j+1}}/(\sqrt{\kappa_j}+\sqrt{\kappa_{j+1}})$. Then by Cauchy-Schwarz inequality and Young inequality, there is

$$
\begin{aligned}
&\sum_{j=1}^{N-1}(\hat{h}(u)[u])_{j+\frac{1}{2}} \\
\geq&\sum_{j=1}^{N-1}\frac{\beta_0}{\Delta x}(\alpha[u]^2)_{j+\frac{1}{2}} - \left\{\sum_{j=1}^{N-1}(\tilde{\kappa}_j\|u_x\|_{I_j}^2 + \tilde{\kappa}_{j+1}\|u_x\|_{I_{j+1}}^2)\right\}^{\frac{1}{2}}\left\{\sum_{j=1}^{N-1}\left(\frac{2C}{\sqrt{\Delta x}}(\sigma[u])_{j+\frac{1}{2}}\right)^2\right\}^{\frac{1}{2}} \\
\geq&\sum_{j=1}^{N-1}\frac{\beta_0}{\Delta x}(\alpha[u]^2)_{j+\frac{1}{2}} - \left\{2\sum_{j=1}^{N}(\tilde{\kappa}_j\|u_x\|_{I_j}^2)\right\}^{\frac{1}{2}}\left\{\sum_{j=1}^{N-1}\left(\frac{2C}{\sqrt{\Delta x}}(\sigma[u])_{j+\frac{1}{2}}\right)^2\right\}^{\frac{1}{2}} \\
\geq&\sum_{j=1}^{N-1}\frac{\beta_0}{\Delta x}(\alpha[u]^2)_{j+\frac{1}{2}} - \varepsilon\sum_{j=1}^{N}(\tilde{\kappa}_j\|u_x\|_{I_j}^2) - \frac{2C^2}{\varepsilon\Delta x}\sum_{j=1}^{N-1}\sigma_{j+\frac{1}{2}}^2[u]_{j+\frac{1}{2}}^2.
\end{aligned}
$$

Replacing the previous estimates into (2.12), there is

$$
\begin{aligned}
B(u,u) \geq&\frac{1}{2}(|||u(\cdot,T)|||^2 - |||u(\cdot,0)|||^2) + \int_0^T\sum_{j=1}^{N}\int_{I_j}(\kappa(x)-\varepsilon\tilde{\kappa}_j)u_x^2 dx dt \\
&+ \int_0^T\sum_{j=1}^{N-1}\left(\frac{\beta_0}{\Delta x}\alpha_{j+\frac{1}{2}} - \frac{2C^2}{\varepsilon\Delta x}\sigma_{j+\frac{1}{2}}^2\right)[u]_{j+\frac{1}{2}}^2 dt \\
&+ \int_0^T(a_1u^2(x_L^+,t) + a_2u^2(x_R^-,t))dt. \qquad (2.13)
\end{aligned}
$$

Taking ε small enough so that $\varepsilon \leq \kappa_0/2\tilde{\kappa}$, then we have $\kappa(x) - \varepsilon\tilde{\kappa}_j \geq \kappa_0/2$. Assuming that

$$
\beta_0 \geq \frac{3C^2}{\varepsilon}\frac{\sigma_{j+\frac{1}{2}}^2}{\alpha_{j+\frac{1}{2}}},
$$

then we get

$$\frac{\beta_0}{\Delta x}\alpha_{j+\frac{1}{2}} - \frac{2C^2}{\varepsilon\Delta x}\sigma^2_{j+\frac{1}{2}} \geq \frac{C^2}{\varepsilon\Delta x}\sigma^2_{j+\frac{1}{2}}.$$

Defining

$$\tilde{\sigma} = \frac{C^2}{\varepsilon}\max_{j=1,\cdots,N-1}\left\{\sigma^2_{j+\frac{1}{2}}\right\},$$

we finally get the estimate for the left hand of (2.11) by (2.13):

$$\begin{aligned} B(u,u) \geq & \frac{1}{2}(|||u(\cdot,T)|||^2 - |||u(\cdot,0)|||^2) + \frac{\kappa_0}{2}\int_0^T \sum_{j=1}^N \int_{I_j} u_x^2 dxdt \\ & + \frac{\tilde{\sigma}}{\Delta x}\int_0^T \sum_{j=1}^{N-1} [u]^2_{j+\frac{1}{2}} dt + \int_0^T (a_1 u^2(x_L^+,t) + a_2 u^2(x_R^-,t))dt. \end{aligned} \tag{2.14}$$

For the right hand side of (2.11), $L(u)$, by using the Hölder inequality and Young inequality, we have

$$\begin{aligned} L(u) = & \int_0^T \sum_{j=1}^N \int_{I_j} f u dx dt + \int_0^T (g_1 u(x_L^+,t) + g_2 u(x_R^-,t))dt \\ \leq & \frac{1}{2}\int_0^T |||f|||^2 dt + \frac{1}{2}\int_0^T |||u(\cdot,t)|||^2 dt + \int_0^T a_1 u^2(x_L^+,t)dt + \int_0^T a_2 u^2(x_R^-,t)dt \\ & + \frac{1}{4a_1}\int_0^T g_1^2(t)dt + \frac{1}{4a_2}\int_0^T g_2^2(t)dt. \end{aligned} \tag{2.15}$$

Replacing (2.14) and (2.15) into (2.11), there is

$$\begin{aligned} & |||u(\cdot,T)|||^2 + \kappa_0 \int_0^T \sum_{j=1}^N \int_{I_j} u_x^2 dx dt + \frac{2\tilde{\sigma}}{\Delta x}\int_0^T \sum_{j=1}^{N-1} [u]^2_{j+\frac{1}{2}} dt \\ \leq & |||u(\cdot,0)|||^2 + \int_0^T |||f|||^2 dt + \frac{1}{2a_1}\int_0^T g_1^2(t)dt \\ & + \frac{1}{2a_2}\int_0^T g_2^2(t)dt + \int_0^T |||u(\cdot,t)|||^2 dt. \end{aligned} \tag{2.16}$$

By the Gronwall inequality

$$\begin{aligned} & |||u(\cdot,T)|||^2 + \kappa_0 \int_0^T \sum_{j=1}^N \int_{I_j} u_x^2 dx dt + \frac{2\tilde{\sigma}}{\Delta x}\int_0^T \sum_{j=1}^{N-1} [u]^2_{j+\frac{1}{2}} dt \\ \leq & C\left(|||u(\cdot,0)|||^2 + \int_0^T |||f|||^2 dt + \frac{1}{2a_1}\int_0^T g_1^2(t)dt + \frac{1}{2a_2}\int_0^T g_2^2(t)dt\right). \end{aligned} \tag{2.17}$$

So we get the stability theorem by the previous estimates as follows.

Theorem 2.1 (L^2 stability). *Consider the DG scheme with numerical flux* (2.6) *for Eq.* (2.1). *Taking the* β_0 *in* (2.6) *large enough, then we get the following estimate*

$$|||u(\cdot,T)|||^2 \le C\left(|||u(\cdot,0)|||^2+\int_0^T |||f|||^2dt+\frac{1}{2a_1}\int_0^T g_1^2(t)dt+\frac{1}{2a_2}\int_0^T g_2^2(t)dt\right). \quad (2.18)$$

2.4. Convergence analysis

We introduce the L^2 projection operator $\mathbb{P}$ from $H^1(\Omega)$ to finite element space V_h satisfying that

$$\int_{I_j}(\mathbb{P}(U)-U)v\,dx=0, \quad \forall v\in V_h. \quad (2.19)$$

Then $u(x,0)=\mathbb{P}(U_0(x))$ by the above projection operator and (2.5). And the projection operator defined by (2.19) satisfies the following estimates.

Lemma 2.1 (L^2 projection properties). *Let* $U\in H^{s+1}(I_j)$, $j=1,\cdots,N$, $s\ge 0$. *Then the following estimates hold*

$$(i)\quad |\mathbb{P}(U)-U|_{m,I_j}\le C\Delta x^{(\min\{k,s\}+1-m)}|U|_{s+1,I_j}, \qquad m\le k+1, \quad (2.20a)$$

$$(ii)\quad |\partial_x^m(\mathbb{P}(U)-U)_{j+\frac{1}{2}}|\le C\Delta x^{(\min\{k,s\}+\frac{1}{2}-m)}|U|_{s+1,I_{j+\frac{1}{2}}}, \quad m\le k+\frac{1}{2}, \quad (2.20b)$$

where m *is nonnegative integer,* $I_{j+\frac{1}{2}}=I_j\bigcup I_{j+1}$, $|\cdot|_{m,I_j}$ *denotes the seminorm of* $H^m(I_j)$.

Lemma 2.2. *Let* U *be the analytical solution of Eq.* (2.1). *Then for the numerical flux* (2.6), *we have*

$$(i)\quad |||(\mathbb{P}(U)-U)(\cdot,T)|||\le C\Delta x^{k+1}|||\partial_x^{k+1}U|||,$$
$$|||(\mathbb{P}(U)-U)_x(\cdot,T)|||\le C\Delta x^{k}|||\partial_x^{k+1}U|||, \quad (2.21a)$$

$$(ii)\quad \int_0^T\sum_{j=1}^{N-1}\hat{h}(\mathbb{P}(U)-U)^2_{j+\frac{1}{2}}dt\le C\Delta x^{2k-1}|||\partial_x^{k+1}U|||^2. \quad (2.21b)$$

Proof. The estimate (2.21a) is easily proved by (2.20a) in Lemma 2.1. For (2.21b) by using (2.20b) in Lemma 2.1, we have

$$\left|\hat{h}(\mathbb{P}(U)-U)_{j+\frac{1}{2}}\right|=\frac{\beta_0}{\Delta x}\alpha_{j+\frac{1}{2}}\left|[\mathbb{P}(U)-U]_{j+\frac{1}{2}}\right|+\beta_{j+\frac{1}{2}}\left|\kappa^-(\mathbb{P}(U)-U)_x^-\right|_{j+\frac{1}{2}}$$
$$+\gamma_{j+\frac{1}{2}}\left|\kappa^+(\mathbb{P}(U)-U)_x^+\right|_{j+\frac{1}{2}}. \quad (2.22)$$

Taking square and summing up for (2.22), we get (2.21b). □

It is easy to verify that the exact solution U of (2.1) also satisfies

$$B(U,v)=L(v), \quad \forall v\in V_h. \quad (2.23)$$

Subtracting (2.23) from (2.9), we obtain the error equation

$$B(u-U,v)=0,\quad \forall v\in V_h. \tag{2.24}$$

In order to obtain the error estimate, we rewrite $e=u-U$ into $e=u-\mathbb{P}(U)+\mathbb{P}(U)-U=\theta-\rho$, where $\theta=u-\mathbb{P}(U)$, $\rho=U-\mathbb{P}(U)$. By triangle inequality, we have

$$|||e|||\le|||\theta|||+|||\rho|||. \tag{2.25}$$

Taking $v=\theta$ in (2.24), we have

$$B(\theta,\theta)=B(\rho,\theta). \tag{2.26}$$

For the left hand side of (2.26), noting that $\theta(x,0)=0$, we get by (2.14)

$$\begin{aligned}B(\theta,\theta)\ge&\frac{1}{2}|||\theta(\cdot,T)|||^2+\frac{\kappa_0}{2}\int_0^T\sum_{j=1}^N\int_{I_j}\theta_x^2dxdt+\frac{\tilde{\sigma}}{\Delta x}\int_0^T\sum_{j=1}^{N-1}[\theta]^2_{j+\frac{1}{2}}dt\\&+\int_0^T(a_1\theta^2(x_L^+,t)+a_2\theta^2(x_R^-,t))dt.\end{aligned} \tag{2.27}$$

For the right hand side of (2.26), we have

$$\begin{aligned}B(\rho,\theta)=&\int_0^T\Big(\sum_{j=1}^N\int_{I_j}\rho_t\theta dx+\sum_{j=1}^N\int_{I_j}\kappa(x)\rho_x\theta_x dx+\sum_{j=1}^{N-1}(\hat{h}(\rho)[\theta])_{j+\frac{1}{2}}\Big)dt\\&+\int_0^T\big(a_1\rho(x_L^+,t)\theta(x_L^+,t)+a_2\rho(x_R^-,t)\theta(x_R^-,t)\big)dt\\=&T_1+T_2+T_3+T_4.\end{aligned}$$

We estimate T_1, T_2, T_3, T_4 in the following, respectively.

Firstly, when $\theta\in V_h$, we have that $T_1=\int_0^T\sum_{j=1}^N\int_{I_j}\rho_t\theta dxdt=0$ by using (2.19).

Secondly, by using the $Hlder$ inequality and Young inequality, we have

$$\begin{aligned}T_2=&\int_0^T\sum_{j=1}^N\int_{I_j}\kappa(x)\rho_x\theta_x dxdt\le\int_0^T\sum_{j=1}^N\int_{I_j}\tilde{\kappa}_j\rho_x\theta_x dxdt\\\le&\int_0^T\sum_{j=1}^N\int_{I_j}\Big(\frac{\kappa_0}{2}\theta_x^2+\frac{\tilde{\kappa}_j^2}{2\kappa_0}\rho_x^2\Big)dxdt\le\frac{\kappa_0}{2}\int_0^T|||\theta_x|||^2dt+\frac{\tilde{\kappa}^2}{2\kappa_0}\int_0^T|||\rho_x|||^2dt.\end{aligned}$$

Then

$$T_3=\int_0^T\sum_{j=1}^{N-1}(\hat{h}(\rho)[\theta])_{j+\frac{1}{2}})dt\le\frac{\tilde{\sigma}}{\Delta x}\int_0^T\sum_{j=1}^{N-1}[\theta]^2_{j+\frac{1}{2}}dt+\frac{\Delta x}{4\tilde{\sigma}}\int_0^T\sum_{j=1}^{N-1}\hat{h}(\rho)^2_{j+\frac{1}{2}}dt.$$

Finally

$$T_4 = \int_0^T \big(a_1\rho(x_L^+,t)\theta(x_L^+,t) + a_2\rho(x_R^-,t)\theta(x_R^-,t)\big)dt$$
$$\le \int_0^T \big(a_1\theta^2(x_L^+,t) + a_2\theta^2(x_R^-,t)\big)dt + \int_0^T \Big(\frac{a_1}{4}\rho^2(x_L^+,t) + \frac{a_2}{4}\rho^2(x_R^-,t)\Big)dt.$$

Replacing T_1, T_2, T_3, T_4 estimations and the inequality (2.27) into (2.26), we get

$$|||\theta(\cdot,T)|||^2 \le \frac{\tilde{\kappa}^2}{\kappa_0}\int_0^T |||\rho_x|||^2 dt + \frac{\Delta x}{2\tilde{\sigma}}\int_0^T \sum_{j=1}^{N-1} \hat{h}(\rho)^2_{j+\frac{1}{2}}\, dt$$
$$+ \int_0^T \Big(\frac{a_1}{2}\rho^2(x_L^+,t) + \frac{a_2}{2}\rho^2(x_R^-,t)\Big)dt. \tag{2.28}$$

By Lemma 2.2, we have

$$|||\theta(\cdot,T)|||^2 \le C\Delta x^{2k}|||\partial_x^{k+1}U|||^2. \tag{2.29}$$

At last (2.25), (2.29) and Lemma 2.2 give the error estimate:

Theorem 2.2 (Convergence). *The numerical solution u of the semi-discrete DG scheme* (2.5) *and the exact solution U of Eq.* (2.1) *satisfy the following error estimate,*

$$|||e(\cdot,T)||| \le C\Delta x^k|||\partial_x^{k+1}U|||. \tag{2.30}$$

3. DG scheme for 2D problem

In this section, we consider the 2-dimensional parabolic equation,

$$\rho c\frac{\partial U}{\partial t} - \nabla\cdot(\kappa(x,y)\nabla U) = f(x,y,t), \quad (x,y)\in\Omega, \quad t>0 \tag{3.1}$$

with boundary conditions,

$$aU + b\kappa(x,y)\frac{\partial U}{\partial n} = g,$$

and initial condition,

$$U(x,y,0) = U_0(x,y),$$

where $0<\kappa_0\le\kappa(x,y)$, ρ, c are defined as same as in 1D case. We take Robin boundary condition by setting $b=1, a>0$. Ω denotes a bounded convex domain in $\mathbb{R}^2$ and $\Omega = \Omega_1\bigcup\Omega_2$, $\Omega_1\bigcap\Omega_2 = \Gamma$. The diffusive coefficient $\kappa(x,y)$ is smooth in Ω_1,Ω_2 respectively but has discontinuity on Γ,

$$\kappa(x,y) = \begin{cases} \kappa_1(x,y), & (x,y)\in\Omega_1, \\ \kappa_2(x,y), & (x,y)\in\Omega_2, \end{cases}$$

and satisfying the following joint condition

$$[U]_\Gamma = 0, \quad \left[\kappa \frac{\partial U}{\partial n}\right]_\Gamma = 0. \tag{3.2}$$

There is a unique solution of Eq. (3.1) satisfying (3.2). We assume the exact solution is smooth enough locally on each subdomain.

3.1. DG scheme

Let $\tilde{\Omega}_1$, $\tilde{\Omega}_2$ be polygonal approximation of Ω_1, Ω_2 and $\tilde{\Omega}_1 \bigcap \tilde{\Omega}_2 = \Gamma_h$. Assume that $\mathscr{T}_{h,1}$, $\mathscr{T}_{h,2}$ are shape-regular triangulation of $\tilde{\Omega}_1$, $\tilde{\Omega}_2$ and $\mathscr{T}_h = \mathscr{T}_{h,1} \bigcup \mathscr{T}_{h,2}$. We assume that the partition is aligned with the interface Γ_h. Let $E \in \mathscr{T}_h$ and Δ_E denotes the diameter of the element E, and the mesh size Δ is given by $\Delta = \max_{E\in\mathscr{T}_h}\{\Delta_E\}$. We denote by $\mathscr{E}_h^o$ the set of all interior edges of $\mathscr{T}_h$ and by $\mathscr{E}_h^\partial$ the set of all boundary faces of $\mathscr{T}_h$ and set $\mathscr{E}_h = \mathscr{E}_h^o \bigcup \mathscr{E}_h^\partial$. Define the DG approximation space as

$$V_h = \{v \in L^2(\Omega) : v|_E \in P^k(E),\ \forall E \in \mathscr{T}_h\}, \tag{3.3}$$

where $P^k(E)$ is a set of polynomials of degree less than or equal to k on element E.

The DG scheme of problem (3.1) can be written as: find $u \in V_h$, for all test functions $v \in V_h$, there are

$$\int_E u_t v dx dy + \int_E \kappa \nabla u \cdot \nabla v dx dy - \int_{\partial E} \hat{h}_u v ds = \int_E f v dx dy, \tag{3.4a}$$

$$\int_E u(x,y,0) v dx dy = \int_E U_0(x,y) v dx dy, \tag{3.4b}$$

where $\hat{h}_u$ in (3.4) is a numerical flux. Let $e \in \mathscr{E}^o$ be an interior face shared by two neighboring elements E_1^e and E_2^e. Denoting by w_1^e and w_2^e the trace of $w(x,y)$ on face e taken from within E_1^e and E_2^e respectively. We define the jump of w at $(x,y) \in e$ by $[w] = w_2^e - w_1^e$. Assume that the unit normal vector $\mathbf{n}$ on boundary e denote oriented from E_1^e to E_2^e. Then the numerical flux on common edge e is defined as

$$\hat{h}_u = \hat{h}(u_1^e, u_2^e, \mathbf{n}) = \frac{\beta_0}{\Delta_e}\alpha_e[u] + \beta_e(\kappa\nabla u \cdot \mathbf{n})_2^e + \gamma_e(\kappa\nabla u \cdot \mathbf{n})_1^e, \tag{3.5}$$

where

$$\alpha_e = \frac{\sqrt{\kappa_1\kappa_2}}{\sqrt{\kappa_1}+\sqrt{\kappa_2}}\max(\sqrt{\kappa_1}, \sqrt{\kappa_2}), \quad \beta_e = \frac{\sqrt{\kappa_1}}{\sqrt{\kappa_1}+\sqrt{\kappa_2}}, \quad \gamma_e = \frac{\sqrt{\kappa_2}}{\sqrt{\kappa_1}+\sqrt{\kappa_2}}.$$

We denote Δ_e as the maximum diameter of two neighboring cells sharing face e and denote κ_1, κ_2 as the values of $\kappa(x,y)$ on the center of element E_1^e and E_2^e respectively. If $e \in \mathscr{E}_h^\partial$, we define a numerical flux as $\hat{h}_u = g - au$. Then the numerical flux (3.5) is consistent with the flux condition (3.2). The numerical flux is also conservative because $\hat{h}_u$ is single-valued on interface. The proof of the numerical solution stability and error analysis is as follows.

3.2. Stability and error analysis

Analogous to the 1D case, we define the norm $|||u|||^2 = \sum_{E\in\mathscr{T}_h}\int_E u^2 dxdy$. Summing up for the equalities (3.4) over all elements and integrating over $[0,T]$, we have the following identity:

$$B(u,v) = L(v), \quad \forall v \in V_h, \tag{3.6}$$

where

$$\begin{aligned} B(u,v) = \int_0^T \Big(\sum_{E\in\mathscr{T}_h}\int_E u_t v dxdy + \sum_{E\in\mathscr{T}_h}\int_E \kappa\nabla u\cdot\nabla v dxdy \\ + \sum_{e\in\mathscr{E}_h^o}\int_e \hat{h}_u[v]ds + \sum_{e\in\mathscr{E}_h^\partial}\int_e auv ds\Big)dt, \\ L(v) = \int_0^T \Big(\sum_{E\in\mathscr{T}_h}\int_E fv dxdy + \sum_{e\in\mathscr{E}_h^\partial}\int_e gv ds\Big)dt. \end{aligned}$$

Set $v = u$ in (3.6). Then there has

$$\begin{aligned} \frac{1}{2}|||u(\cdot,T)|||^2 - \frac{1}{2}|||u(\cdot,0)|||^2 + \int_0^T \Big(\sum_{E\in\mathscr{T}_h}\int_E \kappa(\nabla u)^2 dxdy\Big)dt + \int_0^T \Big(\sum_{e\in\mathscr{E}_h^o}\int_e \hat{h}_u[u]ds\Big)dt \\ + \int_0^T \Big(\sum_{e\in\mathscr{E}_h^\partial}\int_e au^2 ds\Big)dt = \int_0^T \Big(\sum_{E\in\mathscr{T}_h}\int_E fu dxdy + \sum_{e\in\mathscr{E}_h^\partial}\int_e gu ds\Big)dt. \end{aligned} \tag{3.7}$$

We first give a estimate of the fourth term on the left hand side of (3.7). By using the definition of numerical flux (3.5) and trace inequality, we have

$$\begin{aligned} \int_e \hat{h}_u[u]ds &= \int_e \frac{\beta_0}{\Delta_e}\alpha_e[u]^2 + \left(\beta_e(\kappa\nabla u\cdot\mathbf{n})_2^e + \gamma_e(\kappa\nabla u\cdot\mathbf{n})_1^e\right)[u]ds \\ &\geq \int_e \frac{\beta_0}{\Delta_e}\alpha_e[u]^2 ds - \left(\beta_e\|(\kappa\nabla u\cdot\mathbf{n})_2^e\|_{L^2(e)} + \gamma_e\|\kappa(\nabla u\cdot\mathbf{n})_1^e\|_{L^2(e)}\right)\|[u]\|_{L^2(e)} \\ &\geq \int_e \frac{\beta_0}{\Delta_e}\alpha_e[u]^2 ds - C\Big(\frac{\beta_e\tilde{\kappa}_2}{\sqrt{\Delta e}}\|\nabla u\|_{L^2(E_2^e)} + \frac{\gamma_e\tilde{\kappa}_1}{\sqrt{\Delta e}}\|\nabla u\|_{L^2(E_1^e)}\Big)\|[u]\|_{L^2(e)} \\ &\geq \int_e \frac{\beta_0}{\Delta_e}\alpha_e[u]^2 ds - C\frac{2\sigma_e}{\sqrt{\Delta e}}\left(\tilde{\kappa}_2\|\nabla u\|_{L^2(E_2^e)}^2 + \tilde{\kappa}_1\|\nabla u\|_{L^2(E_1^e)}^2\right)^{\frac{1}{2}}\|[u]\|_{L^2(e)}, \end{aligned}$$

where

$$\sigma_e = \frac{\sqrt{\tilde{\kappa}_1\tilde{\kappa}_2}}{\sqrt{\kappa_1}+\sqrt{\kappa_2}}, \quad \tilde{\kappa}_1 = \max_{(x,y)\in E_1^e}\{\kappa(x,y)\}, \quad \tilde{\kappa}_2 = \max_{(x,y)\in E_2^e}\{\kappa(x,y)\}.$$

Denote $\tilde{\kappa}_E = \max_{(x,y)\in E}\{\kappa(x,y)\}$ and $\tilde{\kappa} = \max_{E\in\mathscr{T}_h}\{\tilde{\kappa}_E\}$. By the triangle inequality and *Young* inequality, we get

$$\begin{aligned}
&\sum_{e\in\mathscr{E}_h^o}\int_e \hat{h}_u[u]ds\\
&\geq \sum_{e\in\mathscr{E}_h^o}\frac{\beta_0}{\Delta_e}\alpha_e\|[u]\|^2_{L^2(e)} - C\Big\{\sum_{e\in\mathscr{E}_h^o}(\tilde{\kappa}_2\|\nabla u\|^2_{L^2(E_2^e)} + \tilde{\kappa}_1\|\nabla u\|^2_{L^2(E_1^e)})\Big\}^{\frac{1}{2}}\Big\{\sum_{e\in\mathscr{E}_h^o}\frac{4\sigma_e^2}{\Delta e}\|[u]\|^2_{L^2(e)}\Big\}^{\frac{1}{2}}\\
&\geq \sum_{e\in\mathscr{E}_h^o}\frac{\beta_0}{\Delta_e}\alpha_e\|[u]\|^2_{L^2(e)} - C\Big\{\sum_{E\in\mathscr{T}_h}2\tilde{\kappa}_E\|\nabla u\|^2_{L^2(E)}\Big\}^{\frac{1}{2}}\Big\{\sum_{e\in\mathscr{E}_h^o}\frac{4\sigma_e^2}{\Delta e}\|[u]\|^2_{L^2(e)}\Big\}^{\frac{1}{2}}\\
&\geq \sum_{e\in\mathscr{E}_h^o}\Big(\frac{\beta_0}{\Delta_e}\alpha_e - \frac{2\sigma_e^2C^2}{\varepsilon\Delta e}\Big)\|[u]\|^2_{L^2(e)} - \sum_{E\in\mathscr{T}_h}\varepsilon\tilde{\kappa}_E\|\nabla u\|^2_{L^2(E)}.
\end{aligned}$$

Replacing the above estimate into (3.7) and by the *Hlder* inequality and Young inequality, we obtain

$$\begin{aligned}
&\frac{1}{2}|||u(\cdot,T)|||^2 - \frac{1}{2}|||u(\cdot,0)|||^2 + \int_0^T\sum_{E\in\mathscr{T}_h}\int_E(\kappa-\varepsilon\tilde{\kappa}_E)(\nabla u)^2dxdydt\\
&\qquad + \int_0^T\sum_{e\in\mathscr{E}_h^o}\Big(\frac{\beta_0}{\Delta_e}\alpha_e - \frac{2\sigma_e^2}{\varepsilon\Delta e}\Big)\|[u]\|^2_{L^2(e)}dt\\
\leq&\frac{1}{2}\int_0^T|||f|||^2dt + \frac{1}{2}\int_0^T|||u(\cdot,t)|||^2dt + \int_0^T\sum_{e\in\mathscr{E}_h^\partial}\int_e\frac{g^2}{4a}dsdt.
\end{aligned}$$

Taking ε small enough so that $\kappa_0 - \varepsilon\tilde{\kappa}\geq 0$ and β_0 large enough so that

$$\frac{\beta_0}{\Delta_e}\alpha_e - \frac{2\sigma_e^2}{\varepsilon\Delta e}\geq 0,$$

we complete the proof of stability of the DG scheme (3.4) by the Gronwall inequality.

Theorem 3.1 (L^2 stability)**.** *Assume that β_0 is large enough in numerical flux* (3.5)*. Then the numerical solution of* (3.4) *satisfies*

$$|||u(\cdot,T)|||^2 \leq C\bigg(|||u(\cdot,0)|||^2 + \int_0^T|||f|||^2dt + \int_0^T\sum_{e\in\mathscr{E}_h^\partial}\int_e\frac{g^2}{2a}dsdt\bigg). \tag{3.8}$$

Theorem 3.2 (Error analysis)**.** *Assume that U is the exact solution of* (3.1) *and u is the numerical solution of* (3.4)*. Set that $e = u - U$. Then the following a priori error estimate holds*

$$|||e(\cdot,T)||| \leq C\Delta^k|||U|||_{H^{k+1}(\mathscr{T}_h)}. \tag{3.9}$$

The proof of Theorem 3.2 is analogous to 1D case and is omitted here.

4. Numerical results

In this section, we apply the new DG method to some examples. The first two examples solve 1D parabolic problems and the third example solves 2D parabolic equation with rough coefficients. We show the high order accuracy of the method through these numerical examples. We also illustrate the capacity which the new DG method captures the sharp gradient. We take $\beta_0 = 4$ for P^1 element and $\beta_0 = 10$ for P^2 element in numerical examples.

Example 4.1. Consider a simple linear problem (2.1) with the Dirichlet boundary condition. The diffusion coefficients are defined as follows

$$\kappa(x) = \begin{cases} 0.1 - 0.09x, & x \in \left[0, \frac{2}{3}\right], \\ 0.01, & x \in \left(\frac{2}{3}, 1\right]. \end{cases}$$

The boundary conditions are $U(0,t) = U(1,t) = 0$. The exact solution is

$$U(x,t) = \begin{cases} \exp(-0.1\pi^2 t)\sin(\pi x), & (x,t) \in \left[0, \frac{2}{3}\right] \times (0,T], \\ \exp(-0.1\pi^2 t)\sin(4\pi x), & (x,t) \in \left(\frac{2}{3}, 1\right] \times (0,T]. \end{cases}$$

The initial condition can be derived directly with the exact solution, and the source term $f(x,t)$ can be derived by substituting the exact solution and the diffusion coefficients into the original problem (2.1). Numerical results at $T = 0.1$ are presented in Table 1. It shows optimal 2^{nd} order accuracy for P^1 approximation and 2^{nd} order convergence for P^2 approximation. However the error magnitude of P^2 approximation is less than that of P^1 approximation. The result is plotted in Fig. 1 from 0 to 1 in time t.

Table 1: The error analysis for Example 4.1.

N	P^1 element		P^2 element	
	L_2 error	order	L_2 error	order
15	1.02E-002		6.56E-004	
30	2.64E-003	1.95	1.62E-004	2.02
60	6.68E-004	1.98	4.07E-005	1.99
120	1.68E-004	1.99	1.02E-005	2.00

Example 4.2. Now consider problem (2.1) with Neumann boundary condition. The diffusion coefficients, initial conditions and right term are

$$\kappa(x) = \begin{cases} \frac{4}{9}, & x \in [0,\pi], \\ 4, & x \in (\pi, 2\pi], \end{cases} \qquad \frac{\partial U}{\partial x}(0,t) = \frac{\partial U}{\partial x}(1,t) = 0, \quad f = 0.$$

Then the exact solution is

$$U(x,t) = \begin{cases} \exp(-4t)\cos(3x), & (x,t) \in [0,\pi] \times (0,T], \\ \exp(-4t)\cos(x), & (x,t) \in (\pi, 2\pi] \times (0,T]. \end{cases}$$

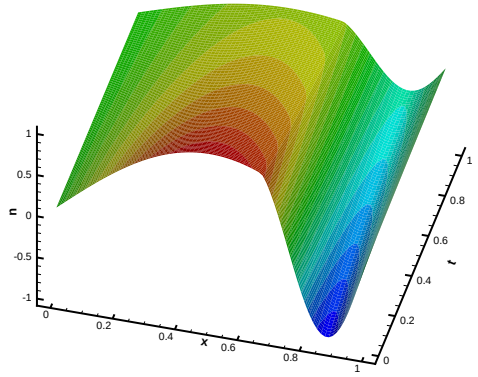

Figure 1: Numerical result for Example 4.1 in $0 \le t \le 1$.

The error and convergence order are listed in Table 2 at $T = 0.1$. We obtain k-th order accuracy for even k and $(k+1)$-th order accuracy for odd k in (2.4).

Table 2: The error analysis for Example 4.2.

N	P^1 element		P^2 element	
	L_2 error	order	L_2 error	order
20	3.65E-002		8.06E-003	
40	9.54E-003	1.94	2.05E-003	1.97
80	2.44E-003	1.97	5.49E-004	1.90
160	5.88E-004	2.05	1.29E-004	2.09

Example 4.3. Consider the 2D problem (3.1) with diffusion coefficient

$$\kappa(x,y) = \begin{cases} d_1, & \sqrt{x^2+y^2} \le 0.5, \\ d_2, & \sqrt{x^2+y^2} > 0.5. \end{cases}$$

The computational domain $\Omega = [-1,1]^2$ and interface is $\Gamma = \{(x,y) : \sqrt{x^2+y^2} = R_1^2\}$. The exact solution of this problem is

$$U(x,y,t) = \begin{cases} e^t\left(\frac{1}{4d_1}(R_1^2 - x^2 - y^2) + \frac{1}{4d_2}(R_2^2 - R_1^2)\right), & \sqrt{x^2+y^2} \le 0.5, \\ \frac{e^t}{4d_2}(R_2^2 - x^2 - y^2), & \sqrt{x^2+y^2} > 0.5. \end{cases}$$

The initial condition and source term $f(x,y,t)$ can be derived according to the above given information. Here we take $R_1 = 0.5$, $R_2 = \sqrt{2}$. The error analysis for P^1 approximation in two cases: $d_1 = 0.1$, $d_2 = 1$ and $d_1 = 0.01$, $d_2 = 1$ at $T = 0.1$ are listed in Table 3. Simulation results verify the correctness of the theoretical analysis. The calculation grid is illustrated in Fig. 2(a). The numerical results at $T = 1$ for different diffusion coefficients are plotted in Figs. 2(b) and (c), respectively. As expected our DG method has the capability to capture the contacts with discontinuous derivatives.

Table 3: The error analysis for Example 4.3.

$\kappa(x,y)$	Number of elements	mesh scale	L^∞ error	L^2 error	L^2 error order
$d_1=0.1,\ d_2=1$	262	2.58E-1	2.28E-2	1.35E-2	-
	968	1.33E-1	7.05E-3	3.83E-3	1.82
	3868	6.78E-2	1.74E-3	9.46E-4	2.02
$d_1=0.01,\ d_2=1$	262	2.58E-1	1.66E-1	9.59E-2	-
	968	1.33E-1	5.53E-2	2.75E-2	1.80
	3868	6.78E-2	1.59E-2	7.03E-3	1.97

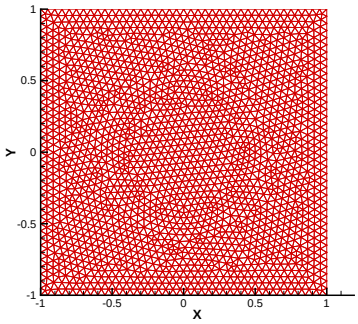

(a) Grid for Example 4.3.

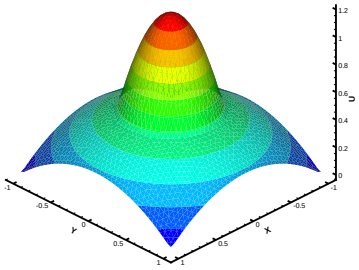

(b) Numerical result with $d_1=0.1,\ d_2=1$.

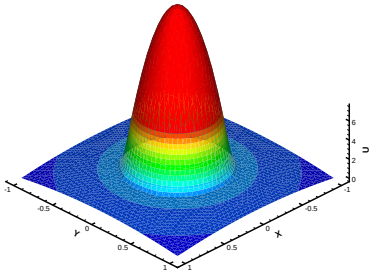

(c) Numerical result with $d_1=0.01,\ d_2=1$.

Figure 2: Grid and numerical result for Example 4.3 at $T=1$.

5. Conclusions

In this paper a new DG method for parabolic equation with discontinuous coefficient is developed. Its stability and convergence properties are proved. The convergent order of numerical solutions is coincided with theoretical analysis. Moreover this method has a fine resolution for sharp gradient. A further work is to extend the DG scheme to nonlinear parabolic equations with jump coefficient.

Acknowledgments This work is supported by the National Natural Science Foundation of China (Grant No: 10771019, 11171038). R. Zhang's work was partially supported by the Young Talent Attraction program of Brazilian National Council for Scientific and

Technological Development (CNPq). The authors would like to thank the referees for their valuable comments and suggestions.

References

[1] G. W. Yuang, X. D. Hang, Z. Q. Sheng and J. Y. Yue, *Progress in numerical methods for radiation diffusion equations*, Chinese J. Comput. Phys., 26 (2009), pp. 475–500.
[2] A. A. Samarskii, Introduction to the Theory of Difference Schemes, Moscow, Nauka, 1971, in Russian.
[3] M. Shashkov and S. Steinberg, *Solving diffusion equations with rough coefficients in rough grids*, J. Comput. Phys., 129 (1996), pp. 383–405.
[4] S. H. Zhu, G. W. Yuang and W. W. Sun, *Convergence and stability of explicit/implicit schemes for parabolic equations with discontinuous coefficients*, Int. J. Numer. Anal. Model., 1 (2004), pp. 131–146.
[5] R. H. Sinha and B. Deka, *Optimal error estimates for linear parabolic problems with discontinuous coefficients*, SIAM J. Numer. Anal., 43 (2005), pp. 733–749.
[6] H. X. Huang and Z. L. Li, *Convergence analysis of the immersed interface method*, IMA J. Numer. Anal., 19 (1999), pp. 583–608.
[7] R. E. Ewing, Z. L. Li, T. Lin and Y. P. Lin, *The immersed finite volume element methods for the elliptic interface problems*, Math. Comput. Simulation, 50 (1999), pp. 63–76.
[8] Z. Li, T. Lin, Y. Lin and R. C. Rogers, *An immersed finite element space and its approximation capability*, Numer. Methods Part. Diff. Eq., 20 (2004), pp. 338–367.
[9] W. H. Reed and T. R. Hill, *Triangular mesh methods for the neutron transport equation*, Los Alamos Scienfic Laboratory Report, LA-UR-73-479, 1973.
[10] B. Cockburn and C. Shu, *TVB Runge-Kutta local projection discontinuous Galerkin finite element methods for conservation laws II: general framework*, Math. Comput., 52 (1989), pp. 411–435.
[11] B. Cockburn, S. Y. Lin and C. Shu, *TVB Runge-Kutta local projection discontinuous Galerkin finite element method for conservation laws III: one-dimensional systems*, J. Comput. Phys., 84 (1989), pp. 90–113.
[12] B. Cockburn and C. Shu, *TVB Runge-Kutta local projection discontinuous Galerkin finite element methods for conservation laws IV: the multidimensional case*, Math. Comput.,54 (1990), pp. 545–581.
[13] B. Cockburn and C. Shu, *TVB Runge-Kutta local projection discontinuous Galerkin finite element methods for conservation laws V: multidimensional systems*, J. Comput. Phys., 141 (1998), pp. 199–224.
[14] B. Cockburn and C. Shu, *The local discontinuous Galerkin method for time-dependent convection-diffusion systems*, SIAM J. Numer. Anal., 35 (1998), pp. 2440–2463.
[15] G. Gassner, F. Lörcher and C. A. Munz, *A contribution to the construction of diffusion fluxes for finite volume and discontinuous Galerkin schemes*, J. Comput. Phys., 224 (2007), pp. 1049–1063.
[16] F. Lörcher, G. Gassner and C. A. Munz, *An explicit discontinuous Galerkin scheme with local time-stepping for general unsteady diffusion equations*, J. Comput. Phys., 227 (2008), pp. 5649–5670.
[17] H. L. Liu and J. Yan, *The direct discontinuous Galerkin (DDG) methods for diffusion problems*, SIAM J. Numer. Anal., 47 (2009), pp. 475–698.
[18] H. L. Liu and J. Yan, *The direct discontinuous Galerkin (DDG) method for diffusion with interface corrections*, Commun. Comput. Phys., 3 (2010), pp. 541–564.

[19] D. A. Pietro and A. Ern, *Analysis of a discontinuous Galerkin method for heterogeneous diffusion problems with low-regularity solutions*, Numer. Methods Part. Diff. Eq., Published online, DOI: 10.1002/num.20675.
[20] A. Ern, A. Stephansen and P. Zunino, *A discontinuous Galerkin method with weighted averages for advection-diffusion equations with locally small and anisotropic diffusivity*, IMA J. Numer. Anal., 29 (2009), pp. 235–256.
[21] A. Ern and A. Stephansen, *A posteriori energy-norm error estimates for discontinuous Galerkin method with weighted averages for advection-diffusion equations approximated by weighted interiori penalty methods*, J. Comput. Math., 26 (2008), pp. 488–510.
[22] Z. Q. Cai, X. Ye and S. Zhang, *Discontinuous Galerkin finite element methods for interface problems: a priori and a posteriori error estimations*, SIAM J. Numer. Anal., to appear.
[23] C. Shu and S. Osher, *Efficient implementation of essentially non-oscillatory shock-capturing schemes*, J. Comput. Phys., 77 (1988), pp. 439–471.